

DEVELOPMENT OF A DIGITAL PILOT
CONTROL MODEL

By

JOHN MARK RICHARDSON

Bachelor of Science

Oklahoma State University

Stillwater, Oklahoma

1975

Submitted to the Faculty of the Graduate College
of the Oklahoma State University
in partial fulfillment of the requirements
for the Degree of
MASTER OF SCIENCE
May, 1977



DEVELOPMENT OF A DIGITAL PILOT
CONTROL MODEL

Thesis Approved:

James K. Rowland

Thesis Adviser

Robert J. Mulholland

Ronald P. Rhee

Norman N. Durham

Dean of the Graduate College

ACKNOWLEDGMENT

I would like to take this opportunity to extend my thanks to Dr. James R. Rowland for his invaluable assistance and guidance throughout this research effort. I also would like to thank Dr. Robert J. Mulholland and Dr. Ronald P. Rhoten for serving on my committee and for their very important contributions to my education.

I was supported during this research period by the United States Air Force Avionics Laboratory under Contract No. F 33615-75-C-1163. Dr. Ronald P. Rhoten was the Project Director and Dr. James R. Rowland was the Task Leader for this research.

Miss Velda Davis and Mrs. Barbara Adams deserve my thanks for their excellent typing of this thesis, and it is heartily extended.

Finally, I wish to thank my parents for their support and encouragement throughout my education.

TABLE OF CONTENTS

Chapter	Page
I. INTRODUCTION	1
Background	2
Preliminary Considerations	5
Thesis Outline	6
II. THE MINIMUM-TIME DETERMINISTIC MODEL	8
Heuristic and Analytic Problem Formulation	8
Optimal Controller Design	12
Numerical Results	18
Summary	19
III. THE STOCHASTIC REGULATOR MODEL	21
Stochastic Problem Formulation	21
Stochastic Controller Design	23
An Application of the Stochastic Controller	27
Summary	32
IV. AN ATTACKER/TARGET AIRCRAFT APPLICATION	33
Description of Attacker Aircraft Model	33
Deterministic Model Results	35
Stochastic Regulator Model Results	38
Summary	43
V. CONCLUSIONS AND RECOMMENDATIONS	44
Conclusions	44
Recommendations for Further Study	45
SELECTED BIBLIOGRAPHY	46

LIST OF FIGURES

Figure	Page
1. A Proposed "Director" Pilot Structure	7
2. A Typical Two-Dimensional Digital Pilot Modeling Problem . .	9
3. Illustration of Attacker and Target Orientations	11
4. Trajectories Resulting from Application of Maximum and Minimum Controls for $B = 0$ and $J = 1$	15
5. An Optimal Trajectory for a Deterministic Minimum-Time Problem	15
6. Determination of the Optimal Trajectory for the System 2.1	16
7. Final Optimization Results for Example Problem	20
8. Control Energy Versus K	29
9. Probability of Target Intercept Versus K	31
10. A Plot of $J(u_K)$ Versus K	31
11. Phase-Plane Trajectories for $u_2 = +0.05$	36
12. Phase-Plane Trajectories for $u_2 = -0.05$	37
13. A Suboptimal Trajectory with Switching at Time t_1	39
14. Description of the Stochastic Minimum-Time Trajectory	42

CHAPTER I

INTRODUCTION

Any dynamic process containing a human as an integral element of that process will, by its very nature, be subject to uncertainties and inconsistencies. Human physical limitations are such that very fast and/or very accurate measurements and decisions are impossible in a process involving humans. The advent of modern high-speed digital computers has made it possible to control processes more rapidly and exactly than was possible with human controllers.

The increased sophistication and reduced cost of digital computers in recent years has resulted in the implementation of digital control algorithms in many areas previously subjected to less exact control. Applications of optimal control theory to many intricate processes has naturally paralleled the strides in the development of digital computers. One result has been the multitude of technological advances made in the area of modern weaponry development and control.

An important area of modern weaponry development in which the human has always been a limiting element is fighter aircraft control in a combat situation. Digital pilot control models have been developed in the past, but when implemented they have failed to perform as well as a human pilot. However, neuro-muscular delays and errors inherent in strictly human decisions, coupled with advances in modern control theory and computer development, provide the impetus to continue

investigation and development of digital pilot model control development .

Background

The need for a satisfactory match of aircraft characteristics and controller properties has been recognized since the inception of aircraft development. Since the aircraft design process does not spontaneously achieve the required man-machine integration, an analytical approach to aircraft stability and control has always been desired. Because of the adaptability of a human controller and his ability to learn, the mathematical investigation of controlled motion has been rendered almost impossible.

A general, quantitative theory was needed to implement a structured approach to the manual control of aircraft. The theory of feedback control systems provided this framework for development. World War II provided the impetus for concerted efforts to apply feedback control theory to increasingly more sophisticated aircraft controlled by human pilots.

Tustin (1) extended feedback control theory by introducing the concept of "describing functions," observation noise measurements, and quasi-linear systems in general. He then applied these concepts to actual human operations. The desire for more systematic development and design of aircraft led to much research aimed at determining the dynamic response characteristics of human pilots. The Goodyear Aircraft group of Meade, Diamantides, Cacioppa, and Mayne (2) (3) developed analog computer representations for human pilots. The United States Air Force supported research which used cross-correlation and

cross-spectral techniques to establish human pilot dynamics (4) (5) (6) (7).

The application of feedback control theory prompted the search for transfer functions which would effectively model a human pilot. Hall (5); Kuehnel (8); McRuer and Krendel (9); Seckel, Hall, McRuer and Weir (4); and Elkind (10) employed the technique of using frequency response data, which were obtained by making a power spectral density analysis of recorded time histories of tests, and comparing with given analytical expressions to determine transfer functions of human pilots.

Westbrook and McRuer (11) found that pilot opinion of airframe configuration is correlated with closed-loop performance and thus to transfer function characteristics. This problem was addressed by Ashkenas and McRuer (12), who developed the theory of handling qualities. This theory attempts to define the extent to which pilot opinion affects transfer function characteristics.

Variations in the transfer function of a human pilot in a single degree-of-freedom simulator were measured by Adams and Bergeron (13). Their work included variations in controlled dynamics and control sensitivity with both compensatory and pursuit tracking. Anderson (14) developed a method of predicting pilot model parameters and closed-loop pilot/vehicle performance subjected to random inputs, and McRuer and Graham (15) investigated the influence of controlled-element dynamics and forcing functions on pilot dynamic characteristics.

McRuer and Krendel (7) (9) (16) and McRuer, Ashkenas, and Guerre (17) developed a rather comprehensive mathematical model which describes pilot/vehicle control systems. This mathematical model has been used extensively to estimate human pilot and overall pilot/vehicle

system dynamic response, stability, and average performance in a variety of situations. Durand and Jex (18) applied the model to tracking tasks, and Durand and Teper (19) applied it to flight path control. Frost (20), Muckler and Obermayer (21), and Smith (22) used the developed model for such diverse applications as systems design, booster guidance, and the determination of the limits of manual control.

McRuer and Krendel (23) have reviewed what is known about the human as a dynamic control component. They discuss quasi-linear models for single-loop and multiloop systems and some nonlinear features of human pilot behavior, such as ability to adapt to changes in visual stimuli.

Pilot control models can typically be grouped into one of three categories. First, most pilot control models have been developed using conventional feedback systems analysis. McRuer, Ashkenas and Graham (24) have provided a comprehensive summary of flight control systems using conventional techniques. Second, Anderson (14) used parameter optimization techniques. The form of the pilot model was assumed a priori and the pilot parameters were then adjusted via a parameter optimization scheme to minimize some desired performance measure. Third, conventional optimal control theory has also been utilized to develop and analyze pilot control models. Baron, Kleinman, et al. (25); Kleinman, Baron, and Levison (26) (27); and Kleinman and Baron (28) applied modern control theory to the analysis of pilot/vehicle systems. They used optimal control theory to permit a pure time-delay and observation noise to be given quantities along with plant characteristics. A performance criterion was selected for minimization, and

the results of computer-based optimization procedures were the closed-loop dynamics and system performance.

Although several results have been reported on the development of pilot models, one area requiring further effort is that of investigating target intercept capabilities in simulated flight situations. The emphasis of this research has been on the use of optimal control theory to investigate the development of a pilot control model which will maximize the probability of target intercept.

Preliminary Considerations

The pilot models discussed in this thesis assume initial conditions which are not greatly perturbed from the final gunnery solution. If initial conditions differ too much from final conditions, then the attacking pilot does not have a good opportunity to initiate an offensive maneuver and would not attack. Thus, only small aspect angle, angle-off, and heading/crossing angles are considered in this research.

For a model to accurately portray a controller as complex as a human pilot, it must necessarily consist of several components. First, a dynamical estimator must utilize all appropriate, noise-corrupted inputs to predict not only some future target position, but also a total target trajectory over some realistic time span. This is the action which a human pilot takes in a compensatory tracking situation. The next component must then select the appropriate controls which will cause the attacker to intercept the target somewhere along its predicted trajectory. An attacking human pilot uses his knowledge of his own aircraft capabilities for control selection, so an accurate attacker aircraft model would be included in the second component of

the pilot model. Next, the inherently human characteristics of a pilot must be incorporated into the model. Such qualities as neuro-muscular delays and reaction time would be modeled in this third component, and the output would be applied to the aircraft dynamics. A block diagram of this pilot model is given in Figure 1.

In air-to-air gunnery situations, human pilots are naturally concerned with minimizing the time required for target acquisition while maximizing the probability of actually shooting the target aircraft. These concepts should also be included in a pilot model with a capability for target intercept. This thesis is concerned with the control-select component of the discussed pilot model. Probability of intercept and time are incorporated as performance measures to be optimized in the selection of controls.

Thesis Outline

Two digital pilot models are considered in the following chapters. Chapter II presents the minimum-time deterministic model, which is a simplified version of later models to be discussed. An assumption made in the formulation of this model was that target position is known for all time. This unrealistic assumption is removed in the model discussed in Chapter III. Only noise statistics regarding future target trajectories are assumed known. This second model employs a quadratic performance measure which results in a closed-loop suboptimal controller. These two pilot models are then applied in Chapter IV to equations which model actual in-flight dynamics of an F-8 Crusader fighter aircraft. Conclusions and recommendations for further study are presented in Chapter V.

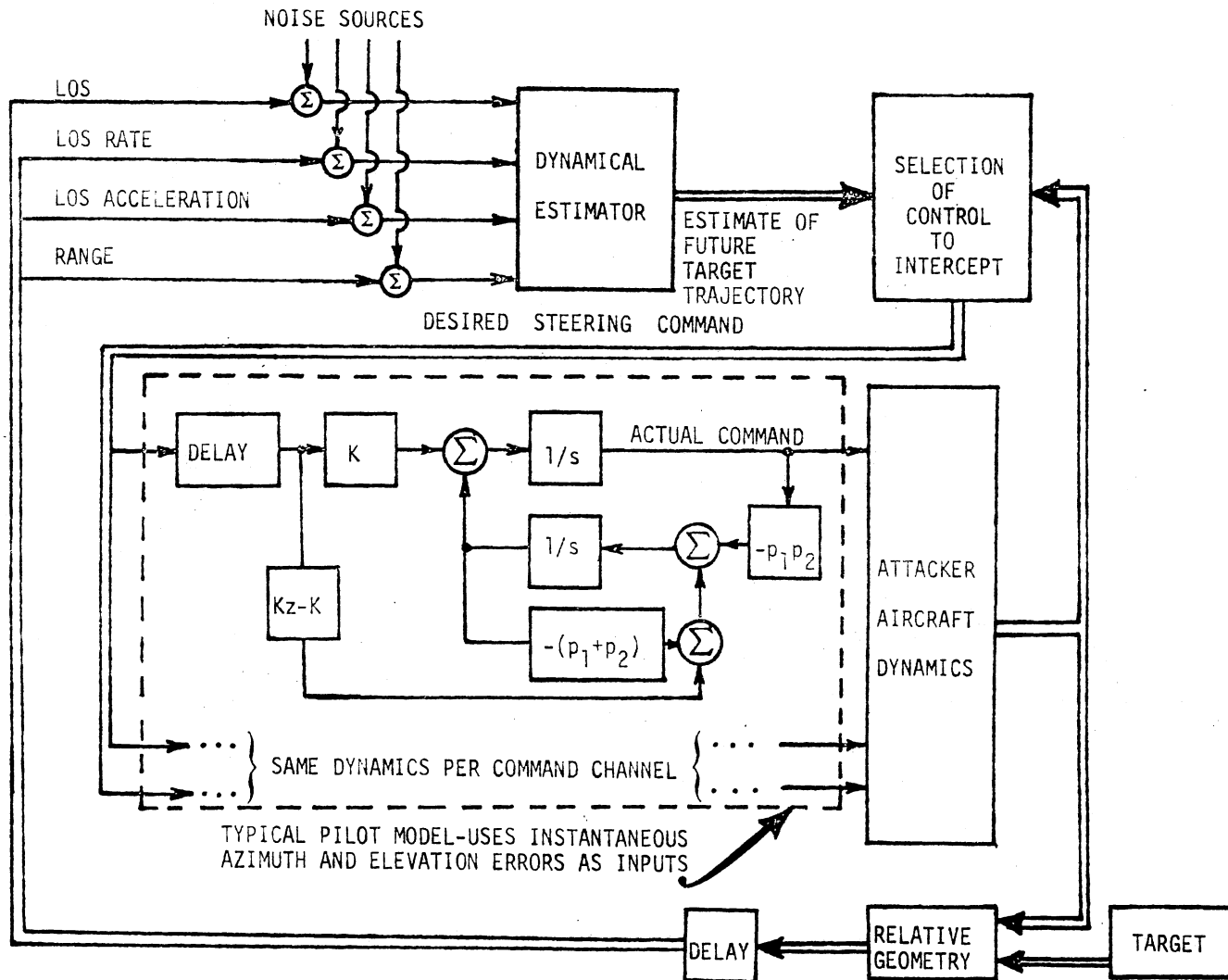


Figure 1. A Proposed "Director" Pilot Structure

CHAPTER II

THE MINIMUM-TIME DETERMINISTIC MODEL

A realistically desirable and intuitively satisfying approach to air-to-air combat is that of target acquisition in minimum time. Using the minimum-time criterion in the formulation of a digital pilot model leads to a well-defined optimal control problem. The optimal control resulting from this formulation is maximum effort during the entire time period. A restricted problem consisting of two-dimensional motion and deterministic target trajectory is presented in this chapter. The mathematical model of this problem is a time-invariant second-order ordinary differential equation. Techniques from optimal control theory are used in the analytical derivation of the optimal controller and results are presented from the application of this controller to the simplified problem implemented on a digital computer.

Heuristic and Analytic Problem Formulation

To illustrate some of the desired properties of the digital pilot model, consider the two-dimensional problem of Figure 2. The target is crossing the attacker's trajectory from left to right and is banked 90° to the left. If a pilot model were used incorporating only line-of-sight error angle θ , the control signal would be to turn left. This control law would lead only to a snap-shoot possibility as the target passed through the attacker's line-of-sight, not to a pointing and

tracking capability as is desired. A slightly more sophisticated model would also utilize the line-of-sight derivative, velocity in the x-direction. This model would result in a turn to the right. However, an actual pilot would be cued visually by the aspect angle that the target, though moving from left to right, was accelerating in the y-direction. If the target pilot maintained the same control strategy, the indicated target trajectory would result with the corresponding attacker trajectory as shown. Thus, it is seen that a human pilot forms an estimate of the target's future trajectory and steers to intercept.

An actual pilot incorporates into his steering command not only target position, but also estimates of target velocity and acceleration. These estimates result in the attacker pilot forming an approximation of the target's future trajectory and thus enables the pilot to steer for pointing and tracking. To be as effective as a human pilot, a digital pilot model must also be provided an estimate of the target's future trajectory.

To indicate how these concepts can be formulated mathematically, consider the two-dimensional problem of attacker and target both flying horizontally and in the same vertical plane with the target aircraft above the attacker aircraft, as in Figure 3. The target trajectory is assumed to be known at every instant of time. Let θ and $\dot{\theta}$ represent the attacker pitch angle and pitch rate and let ϕ and $\dot{\phi}$ represent the angle and angular rate of the target above the attacker. Given knowledge of the future time response of ϕ and $\dot{\phi}$, the intercept problem is to apply control such that $\theta = \phi$ and $\dot{\theta} = \dot{\phi}$ at the earliest possible time. Assuming simple second-order pitch dynamics gives

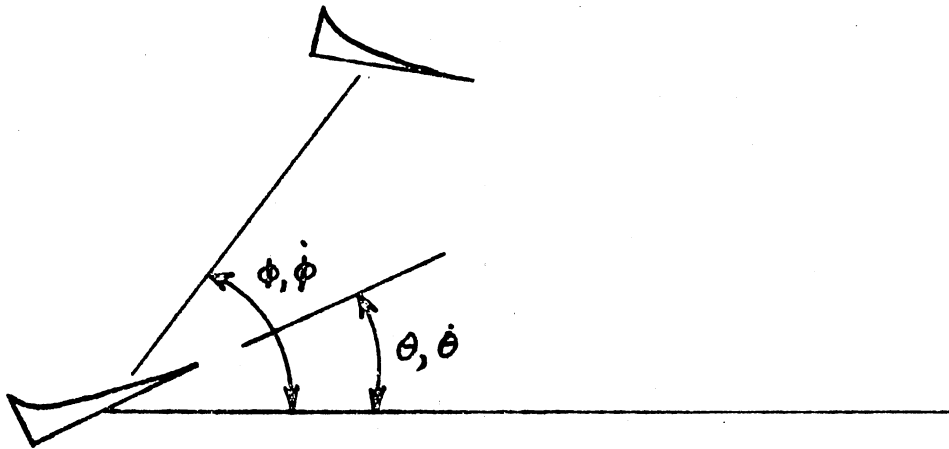


Figure 3. Illustration of Attacker and Target Orientations

$$\frac{\theta(s)}{T(s)} = \frac{1}{s(Js + B)}, \quad (2.1)$$

where J is the rotational inertia of the attacker aircraft, B is the rotational damping of the attacker aircraft, and T is the torque input to the attacker aircraft restricted by $T_{\min} \leq T \leq T_{\max}$. The constants J and B and restrictions on T are determined by the particular aircraft capabilities.

Optimal Controller Design

To facilitate the calculation of the optimal control, standard state-space notation will be used, i.e.

$$\dot{\underline{x}}(t) = A\underline{x}(t) + Bu(t) \quad (2.2)$$

where $\underline{x}(t)$ is the column vector $\begin{pmatrix} x_1(t) \\ x_2(t) \end{pmatrix}$, $\dot{\underline{x}}(t) = \begin{pmatrix} \dot{x}_1(t) \\ \dot{x}_2(t) \end{pmatrix}$, A and B are bounded, continuous matrices, and $u(t)$ is the input control. The solution of Equation 2.2 is well known and is given by

$$\underline{x}(t) = \phi(t - t_0)\underline{x}(t_0) + \int_{t_0}^t \phi(t - \tau)B(\tau)u(\tau)d\tau \quad (2.3)$$

where $\phi(t - \tau)$ is the state transition matrix. The state transition matrix is determined from

$$\phi(t - \tau) = \mathcal{L}^{-1} [(sI - A)^{-1}] \quad (2.4)$$

where \mathcal{L}^{-1} represents the inverse Laplace transform, I is the $n \times n$ identity matrix, and A is the $n \times n$ matrix of Equation 2.2.

Thus, in state space notation, Equation 2.1 becomes

$$\begin{pmatrix} \dot{x}_1(t) \\ \dot{x}_2(t) \end{pmatrix} = \begin{pmatrix} 0 & 1 \\ 0 & -B/J \end{pmatrix} \begin{pmatrix} x_1(t) \\ x_2(t) \end{pmatrix} + \begin{pmatrix} 0 \\ 1/J \end{pmatrix} u(t) \quad (2.5)$$

where $x_1(t) = \theta(t)$, $x_2(t) = \dot{\theta}(t)$, and $u(t) = T$. The state transition matrix for Equation 2.5 is obtained by using Equation 2.4 to form

$$\phi(t - \tau) = \mathcal{L}^{-1} \begin{pmatrix} \frac{1}{s} & \frac{1}{s(s + B/J)} \\ 0 & \frac{1}{s + B/J} \end{pmatrix}$$

which yields

$$\phi(t - \tau) = \begin{pmatrix} 1 & -J/B e^{-B/J(t-t_0)} + J/B \\ 0 & e^{-B/J(t-t_0)} \end{pmatrix}. \quad (2.6)$$

Recalling that the optimal control consists of maximum effort for all $t \geq t_0$, u will always assume the value of either T_{\max} or T_{\min} . Using this fact, Equations 2.3 and 2.6, the solution of Equation 2.5 is given by

$$\begin{pmatrix} x_1(t) \\ x_2(t) \end{pmatrix} = \begin{pmatrix} 1 & -J/B(e^{-B/J(t-t_0)} - 1) \\ 0 & e^{-B/J(t-t_0)} \end{pmatrix} \begin{pmatrix} x_1(t_0) \\ x_2(t_0) \end{pmatrix} + \left\{ \int_{t_0}^t \begin{pmatrix} 1 & -J/B(e^{-B/J(t-\tau)} - 1) \\ 0 & e^{-B/J(t-\tau)} \end{pmatrix} \begin{pmatrix} 0 \\ 1/J \end{pmatrix} d\tau \right\} u(t). \quad (2.7)$$

After integration of Equation 2.7, the solution of Equation 2.5 is

$$\begin{aligned} x_1(t) &= x_1(t_0) + J/B(1 - e^{-B/J(t-t_0)}) x_2(t_0) + \\ &\quad \frac{J}{B^2} (e^{-B/J(t-t_0)})u(t) + \frac{1}{B} (t - t_0)u(t) \\ x_2(t) &= e^{-B/J(t-t_0)} x_2(t_0) + 1/B(1 - e^{-B/J(t-t_0)})u(t). \end{aligned} \quad (2.8)$$

Equations 2.8 provide the trajectories of x_1 and x_2 as functions of time and the initial conditions. However, it is desired to eliminate the time-dependence of the state variables x_1 and x_2 so that a

phase plot may be made. A family of trajectories will result by plotting x_2 versus x_1 with $u = T_{\max}$ and varying the initial conditions. Likewise, a different family of curves will be obtained by letting $u = T_{\min}$. The direction along which the resultant curves are traversed is provided by noticing the values of the state variables as time increases. If these families of curves are plotted in the same phase plane, the optimal trajectory is given from any initial state to any desired final state with at most one switch from $u = T_{\max}$ to $u = T_{\min}$ or $u = T_{\min}$ to $u = T_{\max}$, as illustrated in Figure 4 for $B = 0$ and $J = 1$. Consider, for example, the trajectory for this same case in Figure 5. The initial state is $(x_1(0), x_2(0)) = (2, -1)$, and the desired final state is $(x_1(t_f), x_2(t_f)) = (3, 0)$. The optimal control strategy is to initially apply the control $u = T_{\max}$ until $t = t_1$, then apply the control $u = T_{\min}$ until the desired position is reached.

The stated problem, however, assumes a moving target with known trajectory. Thus, the problem becomes that of determining the switching time such that the attacker trajectory intersects the target trajectory in the phase-plane in minimum time, i.e., from consideration of Figure 6, for general B and J values, determine $t_1 \geq t_0$ such that $t_f \geq t_1$ is minimized.

If one lets $\underline{x}(t, t_0)$ denote the solution of Equation 2.5 with initial condition at t_0 , then for $t_0 \leq t \leq t_1$, Equation 2.8 becomes

$$\begin{aligned}
 x_1(t, t_0) &= x_1(t_0, t_0) + \frac{J}{B} (1 - e^{-B/J(t-t_0)}) x_2(t_0, t_0) + \\
 &\quad \frac{J}{B^2} (e^{-B/J(t-t_0)}) u + \frac{1}{B} (t - t_0)u \\
 x_2(t, t_0) &= e^{-B/J(t-t_0)} x_2(t_0, t_0) + \frac{1}{B} (1 - e^{-B/J(t-t_0)})u . \quad (2.9)
 \end{aligned}$$

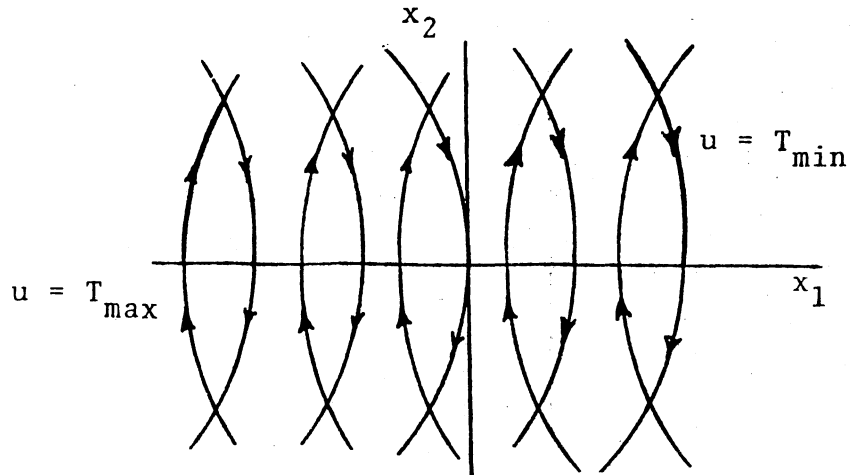


Figure 4. Trajectories Resulting from Application of Maximum and Minimum Control for $B = 0$ and $J = 1$.

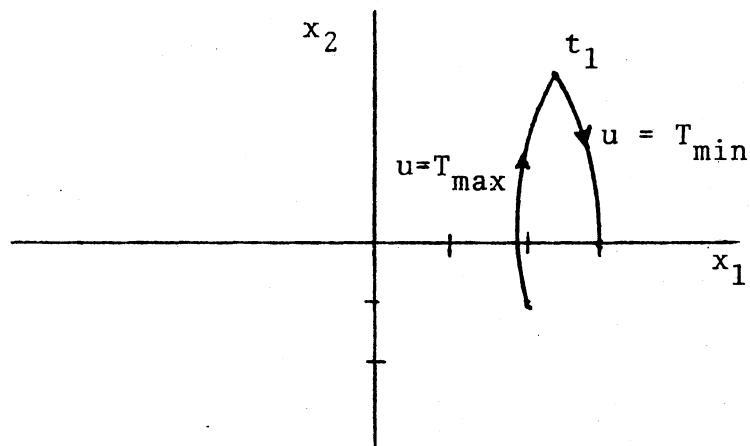


Figure 5. An Optimal Trajectory for a Deterministic Minimum-Time Problem

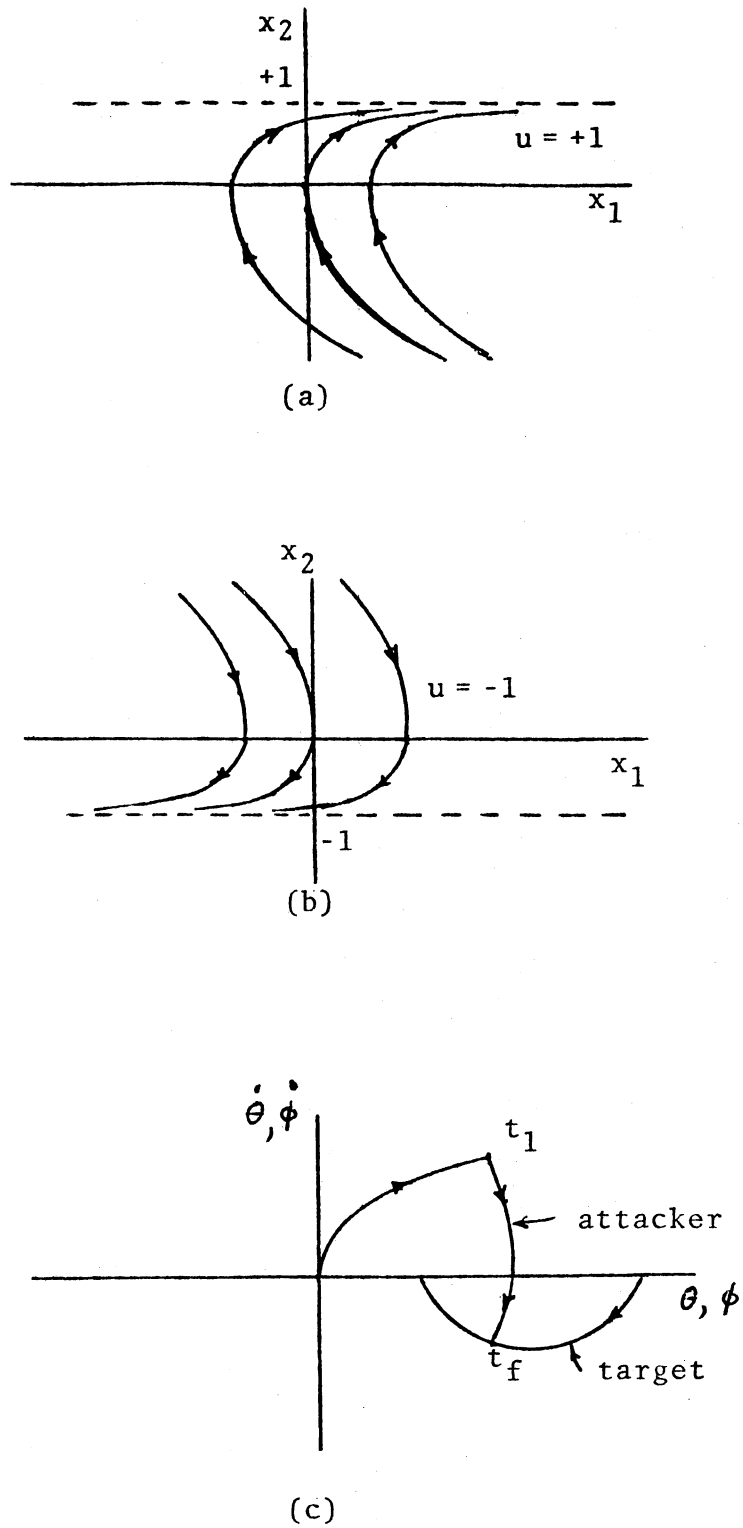


Figure 6. Determination of the Optimal Trajectory for the System 2.1

The solution of Equation 2.5 for $t_1 \leq t \leq t_f$ is

$$\begin{aligned} x_1(t, t_1) &= x_1(t_1, t_1) + \frac{J}{B} (1 - e^{-B/J(t-t_1)}) x_2(t_1, t_1) + \\ &\quad \frac{J}{B^2} (e^{-B/J(t-t_1)}) u + \frac{1}{B} (t - t_1)u \\ x_2(t, t_1) &= e^{-B/J(t-t_1)} x_2(t_1, t_1) + 1/B(1 - e^{-B/J(t-t_1)})u . \end{aligned} \quad (2.10)$$

An iterative gradient method was used for the calculation of t_1 and t_f . Assume a target trajectory designated in the phase plane by $y_1(t)$ and $y_2(t)$ where $y_1 = \phi$ and $y_2 = \dot{\phi}$ and ϕ and $\dot{\phi}$ are as in Figure 3. Then, it is desired to minimize the performance measure $P(t)$ defined by

$$P(t) = [x_1(t_f, t_1) - y_1(t_f)]^2 + [x_2(t_f, t_1) - y_2(t_f)]^2 , \quad (2.11)$$

where t_f represents the time at which the attacker trajectory intersects the target trajectory. The gradient technique is begun by providing an initial value for t_1 and evaluating the performance index $P(t)$. The new value of t_1 , designated as t_{1NEW} , is obtained by expanding $P(t)$ into its Taylor Series and dropping all nonlinear terms.

Thus,

$$P(t)_{NEW} \cong P(t)_{OLD} + \left. \frac{\partial P(t)}{\partial t_1} \right|_{t_f} \Delta t_1 .$$

Assuming that $P(t)_{NEW} = 0$,

$$\Delta t_1 \cong \frac{-P(t)_{OLD}}{\left. \frac{\partial P(t)}{\partial t_1} \right|_{t_f}} .$$

The desired value of t_{1NEW} is then given by

$$t_{1NEW} = t_{1OLD} + \Delta t_1$$

and the technique is repeated until $P(t)$ is minimized.

Numerical Results

Consider the stated problem modeled by Equations 2.9 and 2.10. Assume that $J = 1.0$, $B = 1.0$, $T_{\max} = 1.0$, and $T_{\min} = -1.0$. After implementation of Equations 2.9 on the digital computer and recalling that $u = T_{\max} = 1.0$, the family of trajectories of Figure 6(a) was produced by varying the initial conditions of the state variables x_1 and x_2 . Figure 6(b) shows the family of curves resulting from Equation 2.10 and letting $u = T_{\min} = -1.0$. When these trajectories were plotted in the same phase plane, the optimal path could be found from any initial state to any desired final state, as indicated in Figure 6(c).

To intercept a moving target, the gradient technique discussed in the previous section must be applied. Taking the first partial derivative with respect to t_1 of the performance measure defined by Equation 2.11 yielded

$$\frac{\partial P}{\partial t_1} = 2[x_1(t_2, t_1) - y_1(t_2)] \frac{\partial x_1(t_2, t_1)}{\partial t_1} + 2[x_2(t_2, t_1) - y_2(t_2)] \frac{\partial x_1(t_2, t_1)}{\partial t_1}$$

as the first step in calculating t_1 . The first partial derivatives of $x_1(t_2, t_1)$ and $x_2(t_2, t_1)$ were determined from Equations 2.10 as

$$\frac{\partial x_1(t_2, t_1)}{\partial t_1} = \frac{1}{B} (2 + e^{-B/J(t_1-t_0)} - e^{-B/J(t_2-t_1)}) - (e^{-B/J(t_1-t_0)} + e^{-B/J(t_2-t_1)})$$

$$\frac{\partial x_2(t_2, t_1)}{\partial t_1} = \frac{2}{J} (e^{-B/J(t_2-t_1)}) ,$$

where $u = 1.0$ for $t_0 \leq t < t_1$ and $u = -1.0$ for $t_1 \leq t \leq t_2$.

This system model and iterative gradient technique were simulated on the digital computer with an assumed target trajectory described by

$$\dot{y}_1(t) = -y_1(t) + 5$$

$$\dot{y}_2(t) = -2y_2^2(t) + 24y_2(t) - 70 .$$

Using a fourth-order Runge-Kutta numerical integration algorithm with a step size of 0.1 seconds for an initial condition $(x_1(t_0), x_2(t_0)) = (0, 0)$, the optimal switching time t_1 was calculated to be 7.38 seconds and the elapsed time from the change of control to intercept was determined as 2.8 seconds. The corresponding value of the performance index $P(t)$ was 0.0013. Figure 7 provides the phase plane plot of the aircraft trajectories.

Summary

The minimum time problem for the acquisition and tracking of a target aircraft in an air-to-air combat simulation was solved in two dimensions in this section. It was assumed that the target aircraft trajectory was known, and a method was presented for determining the control strategy necessary for target intercept. In reality, however, the target trajectory will not be known exactly; and the problem will not be restricted to two dimensions. Therefore, the minimum-time formulation of the problem has inherent deficiencies, not only because of the stochastic properties introduced, but also because the geometry of the switching curve becomes prohibitive in more than two dimensions. These considerations lead to the formulation of the stochastic regulator problem, discussed in the following chapter.

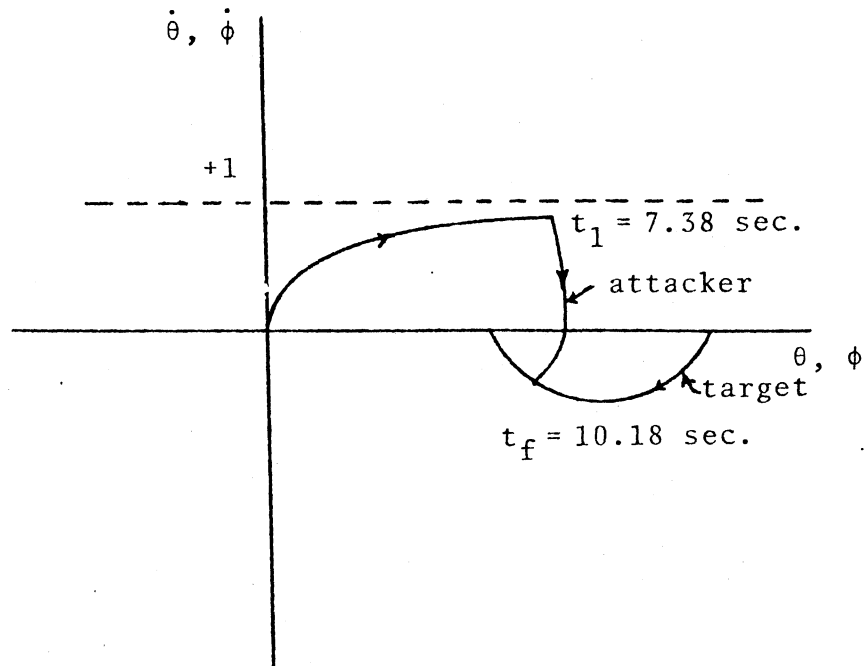


Figure 7. Final Optimization Results for Example Problem

CHAPTER III

THE STOCHASTIC REGULATOR MODEL

Perhaps the most striking limitation of the minimum-time formulation of a digital pilot model is that the target pilot's evasive maneuvers, and therefore his aircraft trajectory, are assumed to be known by the attacker pilot. This is not the case in an actual air-to-air combat situation. Therefore, in complying with the realistic situation, it becomes necessary to include the random nature of the target trajectory in the problem development. Through familiarity with the target aircraft, the attacker pilot can make judgments of worst-case possibilities for the target pilot's evasive actions. The issue concerns maximizing the probability of intercept and not the determination of the point of intercept. Control energy consumption is also of concern in the present formulation of the problem. This chapter deals with the solution and implementation of the stochastic regulator problem.

Stochastic Problem Formulation

The stochastic regulator problem is a problem in optimal control involving the use of a performance measure which includes a probability term. The probability term in this case is a measure of the likelihood of entering a target manifold. Consequently, it indicates the possibility of intercepting a trajectory lying within the manifold. An

energy term to be minimized is also included in the performance index.

Specifically, the system to be controlled is given by

$$\dot{\underline{x}}(t) = A\underline{x}(t) + B\underline{u}(t) + C\underline{w}(t) \quad (3.1)$$

where the state of the system is defined by the n -vector $\underline{x}(t)$; $\underline{u}(t)$ is the control input; $\underline{w}(t)$ is a white noise input; and A , B , and C are all bounded, continuous-time matrices. The performance index which is to be minimized was suggested in (29) as

$$J(\underline{u}) = P \left\{ \min_{t_0 \leq t \leq t_f} \left[\frac{\tilde{\underline{x}}^T(t) \tilde{a}^{-1}(t) \tilde{\underline{x}}(t)}{r(\hat{\underline{x}}(t))} \right] \leq \rho \right\} - \int_{t_0}^{t_f} \underline{u}^T(t) U \underline{u}(t) dt, \quad (3.2)$$

where the upper case T denotes the transpose. In Equation 3.2, P denotes probability and $\hat{\underline{x}}(t)$ and $\tilde{\underline{x}}(t)$ are vectors such that

$$\underline{x}(t) = \begin{bmatrix} \tilde{\underline{x}}(t) \\ \hat{\underline{x}}(t) \end{bmatrix}.$$

$r(\hat{\underline{x}}(t)) \geq 0$ is a bounded, continuous scalar function such that $\tilde{\underline{x}}^T(t) \tilde{a}^{-1}(t) \tilde{\underline{x}}(t) = r(\hat{\underline{x}})$ defines the manifold which bounds the target set. The quantity $\rho \geq 0$ is a constant which specifies the allowable "miss" of the target set. Thus, $\rho \leq 1$ assures penetration of the target manifold. Moreover, \tilde{a} is the nonsingular matrix defined for $t \in (t_0, t_f)$ satisfying

$$C W(t) C^T = \begin{pmatrix} \tilde{a}^{-1}(t) & 0 \\ 0 & 0 \end{pmatrix}, \quad (3.3)$$

where $W(t)$ is a matrix such that

$$E\{\underline{w}(t_1) \underline{w}^T(t_2)\} = W(t) \delta(t_2 - t_1)$$

for $t_2 > t_1$ and $E\{\cdot\}$ denotes the expectation. The requirement of Equation 3.3 involves no loss of generality since it can be attained by a nonsingular transformation.

The matrix U in Equation 3.2 is real, symmetric, and positive definite. The input control vector \underline{u} satisfies the requirement that $\int_{t_0}^{t_f} \underline{u}^T(t) \underline{u}(t) dt < \infty$, where t_0 and t_f are specified constants.

Thus, it is required to choose a control vector \underline{u} which will force the stochastic system described by Equation 3.1 from an initial state $\underline{x}(t_0)$ to a final state $\underline{x}(t_f)$ such that the probability of the system trajectory $\underline{x}(t)$, where $t \in (t_0, t_f)$, entering a target manifold bounded by $\tilde{\underline{x}}^T(t) \tilde{\underline{a}}^{-1}(t) \tilde{\underline{x}}(t) = r(\tilde{\underline{x}})$ is maximized, and the control energy described by $\int_{t_0}^{t_f} \underline{u}^T(t) U(t) \underline{u}(t) dt$ is minimized.

Stochastic Controller Design

The determination of the optimal controller for the stated stochastic regulator problem is rather prohibitive for two reasons. First, no exact, closed-form solution is presently known for the probability term, which is the solution to the Kolmogorov diffusion equation with initial and boundary conditions. Second, even if a closed-form solution were available, the optimal approach would require the solution of a two-point boundary value problem, which is formidable in itself. For these reasons, it becomes desirable to employ a sub-optimal approach to the problem.

The basic idea of the suboptimal solution can be described in three steps. First, a class of controls that minimizes a performance

index containing both the time-average distance from the target manifold and the consumed control energy is determined for the noise-free system. The proportion of the distance to the energy is parameterized by a proportionality constant. Second, for every element in this control class, the probability of the state of the stochastic system entering the target manifold is computed by simulation on the digital computer. Finally, the optimal control in this class is found by a direct search. This resulting control is the desired suboptimal control for the stochastic system.

When the noise disturbances are absent, system 3.1 reduces to the familiar form

$$\dot{\underline{x}}(t) = \underline{A}\underline{x}(t) + \underline{B}\underline{u}(t) . \quad (3.4)$$

Let $J_K(\underline{u})$ define the performance index which includes both the time-averaged distance from the target set and the consumed control energy, with the relative weighting of distance to energy given by the constant K . Then,

$$J_K(\underline{u}) = \int_{t_0}^{t_f} \underline{x}^T(t) \tilde{a}^{-1}(t) \underline{x}(t) + K \underline{u}^T(t) V(t) \underline{u}(t) dt , \quad (3.5)$$

where $K > 0$, $V(t) = U(t) / \left[\max_i \max_j \max_{t_0 \leq t \leq t_f} |U_{ij}(t)| \right]$ and $U_{ij}(t)$ is the element of $U(t)$ in the i -th row and j -th column. Also, for all \underline{u} satisfying the condition $\int_{t_0}^{t_f} \underline{u}^T(t) \underline{u}(t) dt < \infty$, let

$$J_K(\underline{u}_K) \leq J_K(\underline{u}) ,$$

subject to the constraint of the system in Equation 3.4.

It is known that system 3.4 with $J_K(\underline{u})$ defined by Equation 3.5 has the linear closed-loop optimal control

$$\underline{u}_K(x, t) = - \frac{V^{-1}(t) B^T(t) R(t) \underline{x}(t)}{K} \quad (3.6)$$

where $R(t) = R^T(t)$ satisfies the matrix Riccati differential equation

$$-\dot{R}(t) = R(t)A(t) + A^T(t)R(t) - \frac{R(t)B(t)V^{-1}(t)B^T(t)R(t)}{K} + G(t) \quad (3.7)$$

with

$$G(t) = \begin{pmatrix} \tilde{a}^{-1}(t) & 0 \\ 0 & 0 \end{pmatrix} \quad (3.8)$$

and $R(t_f) = 0$. Thus, $R(t)$, for $t \in (t_0, t_f)$, can be computed numerically. Since $R(t)$ can be calculated, $\underline{u}_K(x, t)$, for $t \in (t_0, t_f)$, can be determined for every constant K and for every given initial condition $\underline{x}(t_0)$.

Thus, each control $\underline{u}_K(x, t)$ is an optimal solution to the deterministic system in Equation 3.4 with $J_K(\underline{u})$ given by Equation 3.7, $K > 0$, and the initial conditions $\underline{x}(t_0)$ known. The performance index J_K contains two terms: a time average of the distance $\tilde{\underline{x}}^T(t)\tilde{a}^{-1}(t)\tilde{\underline{x}}(t)$ and a control energy term. Intuitively, making the time average of the distance small makes the probability term of $J(\underline{u})$ large. By letting

$$K = \max_i \max_j \max_{t_0 \leq t \leq t_f} |U_{ij}(t)| ,$$

the control energy terms of both $J_K(\underline{u})$ and $J(\underline{u})$ will be the same. In $J_K(\underline{u})$, however, K is a parameter which determines the relative weight placed on the two terms of $J_K(\underline{u})$. Thus, the parameter K provides an adjustment of the trade-off between the distance and the control energy.

In the digital computer simulation of the model in Equation 3.1,

the input $\underline{w}(t)$ is assumed to be white noise.

A random number generator can thus be used to provide the noise disturbances. Using $\underline{u}_K(x, t)$ as defined by Equation 3.6 for $\underline{u}(t)$ on the interval $t \in (t_0, t_f)$ and a fourth-order Runge-Kutta algorithm (RK4) for integration, $\underline{x}(t)$ can be simulated and computed for every $K > 0$. Let $\underline{x}(t, K)$ denote the digital simulation of $\underline{x}(t)$.

The performance index $J(\underline{u})$ defined by Equation 3.2 contains two terms. The energy term is obtained directly by computing

$$K \int_{t_0}^{t_f} \underline{u}_K^T(t) V(t) \underline{u}_K(t) dt. \quad \text{If}$$

$$K = \max_i \max_j \max_{t_0 \leq t \leq t_f} |U_{ij}(t)|,$$

then this term is identically equal to $\int_{t_0}^{t_f} \underline{u}_K^T(t) U(t) \underline{u}_K(t) dt$.

The estimate of the probability term is carried out by making N Monte Carlo simulations, thereby providing N sample trajectories of $\underline{\tilde{x}}^T(t, K) \tilde{a}^{-1} \underline{\tilde{x}}(t, K)$ for $t \in (t_0, t_f)$. Let

$$\sigma_i = \min_{t_0 \leq t \leq t_f} \left[\frac{\underline{\tilde{x}}_i^T(t, K) \tilde{a}^{-1}(t) \underline{\tilde{x}}_i(t, K)}{r(\underline{\hat{x}}_i(t, K))} \right], \quad i = 1, 2, \dots, N, \quad (3.9)$$

where $\underline{\tilde{x}}_i^T(t, K) \tilde{a}^{-1}(t) \underline{\tilde{x}}_i(t, K)$ is the i -th observed sample trajectory. Denote these N quantities of σ_i by $X(j)$, $j = 1, 2, \dots, N$. These N values are then sorted in a monotonically decreasing order with respect to j . A plot of $(N - j + 1)/N$ versus $X(j)$ is then made and a curve is fitted to the points. This curve represents the least-squares best-fit parabola. The resulting curve represents a plot of the simulated values of

$$P \left\{ \min_{t_0 \leq t \leq t_f} \left[\frac{\underline{\tilde{x}}^T(t, K) \tilde{a}^{-1}(t) \underline{\tilde{x}}(t, K)}{r(\underline{\hat{x}}(t, K))} \right] \leq \rho \right\} \quad (3.10)$$

versus ρ for a given $K > 0$.

Repeating the procedure M times for M different K , a family of M curves can be constructed. Thus, for a specified $\rho = \rho_0$, M values of

$$P \left\{ \min_{t_0 \leq t \leq t_f} \left[\frac{\tilde{\mathbf{x}}^T(t, K) \tilde{\mathbf{a}}^{-1}(t) \tilde{\mathbf{x}}(t, K)}{r(\hat{\mathbf{x}}(t, K))} \right] \leq \rho_0 \right\}$$

with their corresponding values of K can be determined from this family of K curves. For each of the M values of K used, the energy term $K \int_{t_0}^{t_f} \frac{\mathbf{u}_K^T(t)}{K} V(t) \frac{\mathbf{u}_K(t)}{K} dt$ is computed. Thus, by Equation 3.2, the simulated performance index

$$J(\mathbf{u}_K) = P \left\{ \min_{t_0 \leq t \leq t_f} \left[\frac{\tilde{\mathbf{x}}^T(t, K) \tilde{\mathbf{a}}^{-1}(t) \tilde{\mathbf{x}}(t, K)}{r(\hat{\mathbf{x}}(t, K))} \right] \leq \rho_0 \right\} - K \int_{t_0}^{t_f} \frac{\mathbf{u}_K^T(t)}{K} V(t) \frac{\mathbf{u}_K(t)}{K} dt \quad (3.11)$$

can be obtained for each K .

This procedure yields M values of $J(\mathbf{u}_K)$. If one lets $J^* = J(\mathbf{u}_K^*)$ be the maximum value among all M of the $J(\mathbf{u}_K)$, then \mathbf{u}_K^* is the desired suboptimal control for system 3.1, the corresponding K is the optimal choice of the proportionality constant in Equation 3.5, and J^* is the optimal value of the performance index corresponding to the suboptimal control \mathbf{u}_K^* .

An Application of the Stochastic Controller

In order to illustrate the concepts set forth above, consider the stochastic system described by

$$\begin{aligned} \dot{x}_1(t) &= x_2(t) + w_1(t) \\ \dot{x}_2(t) &= -2x_1(t) - 3x_2(t) + u(t) + w_2(t) \end{aligned}$$

with initial conditions $x_1(0) = x_2(0) = 1$. Assuming that $r(\hat{x}) = 0.1$ and $V(t) = 1$ for this problem, it is desired to drive the system from the initial state to the circle centered at the origin with radius equal to 0.1 in the time interval from 0 to 3 seconds. The performance measure associated with the above stated problem is given by

$$J(u) = P \left\{ \min_{0 \leq t \leq 3} \left[\frac{\sqrt{x_1^2(t) + x_2^2(t)}}{0.1} \right] \leq \rho \right\} - \int_0^3 u^2(t) dt$$

where $\tilde{a}^{-1} = \begin{pmatrix} 1 & 0 \\ 0 & 1 \end{pmatrix}$ and $U(t)$ is assumed to be 1. A step size of 0.1 seconds was used for all integrations.

The first step in the determination of the control strategy is to form the performance index for the deterministic system as in Equation 3.5. Then

$$J_K(u) = \int_0^3 (x_1^2(t) + x_2^2(t) + Ku^2(t)) dt$$

and the desired control $u_K(x, t)$ is found from Equation 3.6 as

$$u_K(\underline{x}, t) = -\frac{1}{K} (R_{12}(t)x_1(t) + R_{22}(t)x_2(t))$$

where $R_{ij}(t)$ is the entry in the i -th row and j -th column of the matrix $R(t)$ satisfying Equation 3.7 with $G(t) = \begin{pmatrix} 1 & 0 \\ 0 & 1 \end{pmatrix}$. Thus, the Riccati gains $R_{12}(t)$ and $R_{22}(t)$ must be calculated and stored subject to the final condition $R(3) = 0$. From these values of $R_{12}(t)$ and $R_{22}(t)$, the control $u_K(\underline{x}, t)$ can be found and the energy term of the performance index can be evaluated from the calculations of

$$K \int_0^3 u_K^2(\underline{x}, t) dt .$$

Figure 8 provides the energy terms plotted against K .

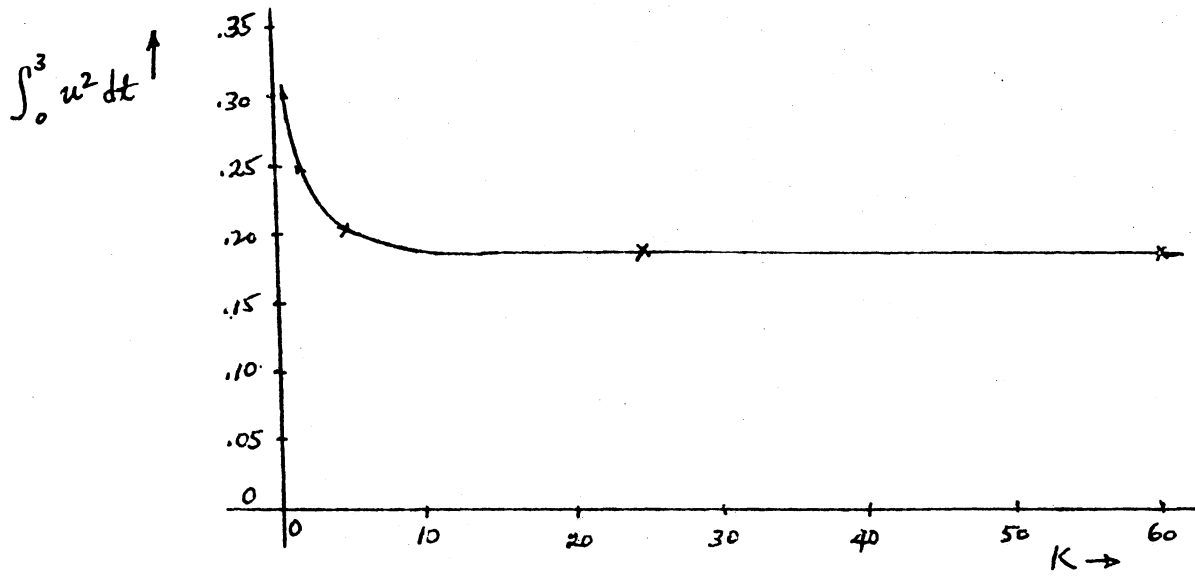


Figure 8. Control Energy Versus K

The estimates of the probability term were carried out by observing 100 sample trajectories of $\sqrt{x_1^2(t) + x_2^2(t)}$ for each of the six values of K , and then defining

$$\sigma_i = \min_{0 \leq t \leq 3} \frac{\sqrt{(x_1^2(t) + x_2^2(t))_i}}{0.1}, \quad i = 1, 2, \dots, 100,$$

where $(x_1^2(t) + x_2^2(t))_i$ is the i -th observed sample trajectory. These 100 values of σ_i were then sorted in monotonically decreasing order and a linear interpolation algorithm was used to determine the probability term

$$P \left\{ \min_{0 \leq t \leq 3} \left[\frac{\sqrt{x_1^2(t) + x_2^2(t)}}{0.1} \right] \leq 3.0 \right\}$$

associated with each value of K and a specified $\rho = 3.0$. These resulting six values of probability were then plotted against the corresponding values of K as shown in Figure 9. Combining Figures 8 and 9 yields the plot of

$$J(u_K) = P \left\{ \min_{0 \leq t \leq 3} \left[\frac{\sqrt{x_1^2(t) + x_2^2(t)}}{0.1} \right] \leq 3.0 \right\} - \int_0^3 u_K^2(t) dt$$

versus K as shown in Figure 10. An examination of this figure shows the maximum value of $J(u_K)$ occurs for $K = 60.0$. The corresponding performance is $J^* = J(u_{60}) = 0.41$ with

$$P \left\{ \min_{0 \leq t \leq 3} \left[\frac{\sqrt{x_1^2(t) + x_2^2(t)}}{0.1} \right] \leq 3.0 \right\} = 0.61$$

and

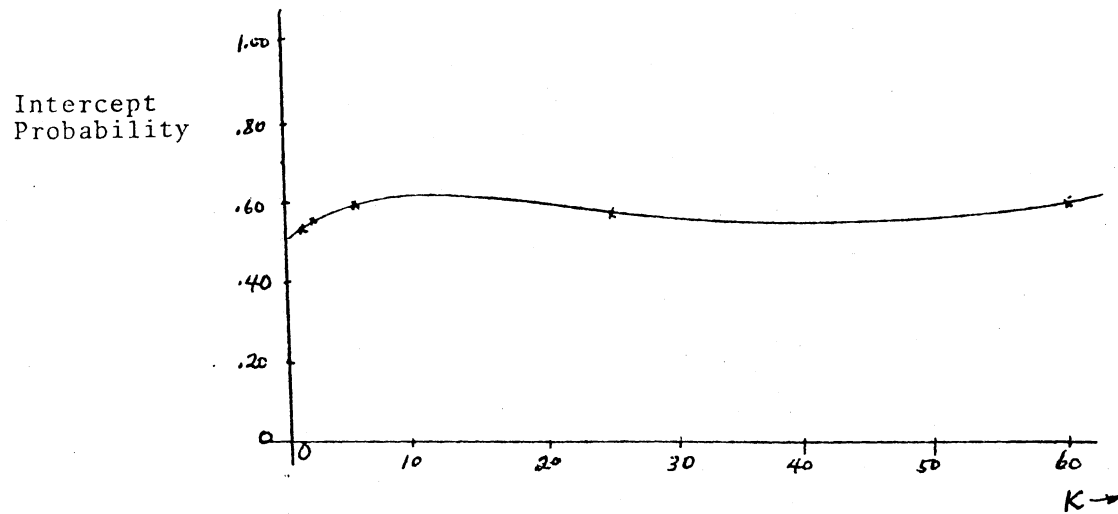


Figure 9. Probability of Target Intercept Versus K

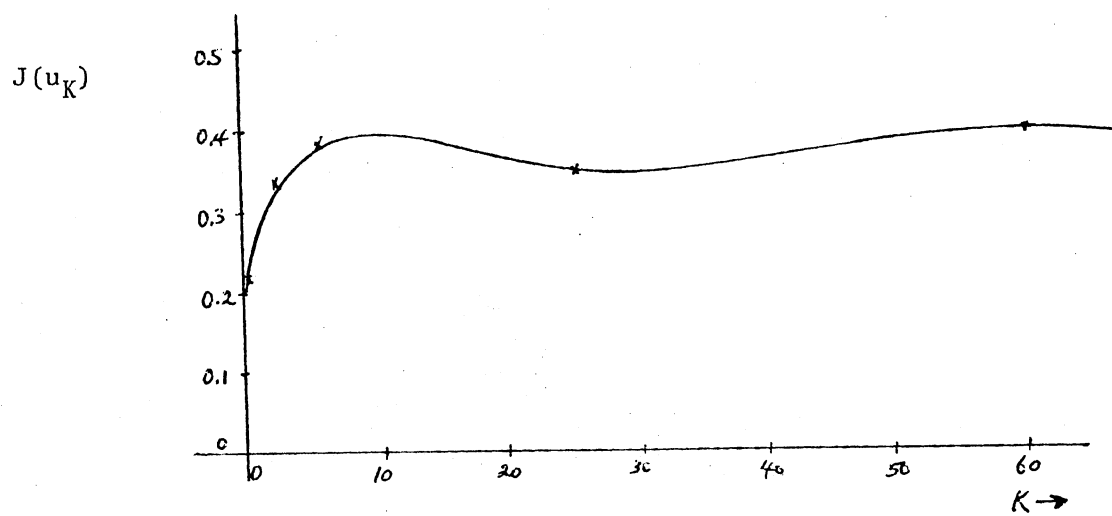


Figure 10. A Plot of $J(u_K)$ Versus K

$$K \int_0^3 u_{60}^2(t) dt = 0.20 .$$

Summary

Considering the unknown behavior of a target pilot results in the necessity of incorporating randomness into the pilot model development. This chapter illustrated the principles involved in designing a stochastic controller concerned with maximizing the probability of intercept and minimizing control energy expenditure. A second-order problem was used as an example. Higher order systems are required to realistically model airplane behavior. The concepts of this chapter are applied in the next chapter to a sixth-order system with noise disturbances, which models an actual aircraft in flight.

CHAPTER IV

AN ATTACKER/TARGET AIRCRAFT APPLICATION

The effectiveness of any developed algorithm for aircraft control is inherently restricted by the accuracy of the particular model used for the simulation. The model employed for the present synthesis problem consists of a sixth-order system of linear differential equations with two control inputs. Because of the practically intractable geometry associated with a sixth-order three-dimensional aircraft model, the present chapter analyzes motion in only one physical dimension. A suboptimal minimum-time deterministic solution is presented in the x-direction and conditions for its validity are discussed. Analysis is also presented leading to the conclusion that the minimum-time formulation provides a useful suboptimal solution for the realistic problem, even if the stochastic framework is used.

Description of Attacker Aircraft Model

The mathematical model used to characterize general aircraft motion employs six equations containing variables which determine aircraft dynamics for any time. It is assumed that all turns are coordinated, implying that there is no sideslip. Also, there are two rate inputs to the aircraft, roll rate and angle-of-attack rate. These inputs are applied through pressure exerted on a control stick in the cockpit, which is then converted into the desired rate inputs.

Using state variable notation, the mathematical model is given

by

$$\begin{bmatrix} \dot{x}_1(t) \\ \dot{x}_2(t) \\ \dot{x}_3(t) \\ \dot{x}_4(t) \\ \dot{x}_5(t) \\ \dot{x}_6(t) \end{bmatrix} = \begin{bmatrix} -.996 & 0 & 0 & 0 & 0 & 0 \\ .021 & 0 & 0 & 0 & 0 & 0 \\ 1 & 0 & 0 & 0 & 0 & 0 \\ 0 & 0 & 0 & -.822 & .002 & 0 \\ 0 & 0 & 0 & 0 & -.083 & -32.163 \\ 0 & 0 & 0 & 1 & 0 & 0 \end{bmatrix} \begin{bmatrix} x_1(t) \\ x_2(t) \\ x_3(t) \\ x_4(t) \\ x_5(t) \\ x_6(t) \end{bmatrix} + \begin{bmatrix} .108 & 0 \\ .999 & 0 \\ 0 & 0 \\ 0 & -94.820 \\ 0 & -93.907 \\ 0 & 0 \end{bmatrix} \begin{bmatrix} u_1(t) \\ u_2(t) \end{bmatrix} \quad (4.1)$$

where $x_1(t)$ is the yaw rate, $x_2(t)$ is the bank angle, $x_3(t)$ is the yaw angle, $x_4(t)$ is the pitch rate, $x_5(t)$ is the velocity, $x_6(t)$ is the pitch angle, $u_1(t)$ is the roll rate input, and $u_2(t)$ is the angle-of-attack rate input. The coefficients are actual numbers obtained from tests using an F8 Crusader aircraft

To provide necessary and useful results, the solutions obtained from Equation 4.1 must be transformed into a coordinate system based on earth positions and velocities. These transformations are obtained by a series of trigonometric equations which result in the velocity vectors of the aircraft in the x-, y-, and z-directions relative to earth. These velocity equations are then integrated to provide

position in the x-, y-, and z-directions in earth coordinates. All initial conditions were assumed to be zero, except velocity in the x-direction and altitude. Initial velocity in the x-direction was chosen to be 700 feet per second, which is approximately 480 miles per hour, a realistic velocity for an actual combat situation. Initial altitude was chosen to be 12,000 feet.

Deterministic Model Results

For the deterministic minimum-time solution of the problem, bounds on the inputs $u_1(t)$ and $u_2(t)$ were chosen. The roll rate was required to be less than or equal to $\pi/2$ radians per second and the angle-of-attack rate was required to be less than or equal to 0.05 radians per seconds. The optimal solution for the minimum-time problem is known to be maximum or minimum input for the entire time interval. However, the realistic situation requires that angle-of-attack be somewhat less than 10° . Also, a roll rate of $\pi/2$ radians would be applied for only a short period of time. Thus, the solution in the real situation is initially to apply maximum input for a short time, then apply no control until a switching time occurs. Then, apply minimum control for a short time and change to no control until intercept.

Applying maximum control for the first one-half second results in the phase plane trajectories in the x-plane shown in Figure 11. Angle-of-attack rate was 0.05 radians per second for the first one-half second of flight. Roll rate had no influence in the x-plane. Figure 12 provides trajectories for an angle-of-attack rate equal to -0.05 radians per second for the first one-half second of flight. The trajectories provided are for five seconds of flying time.

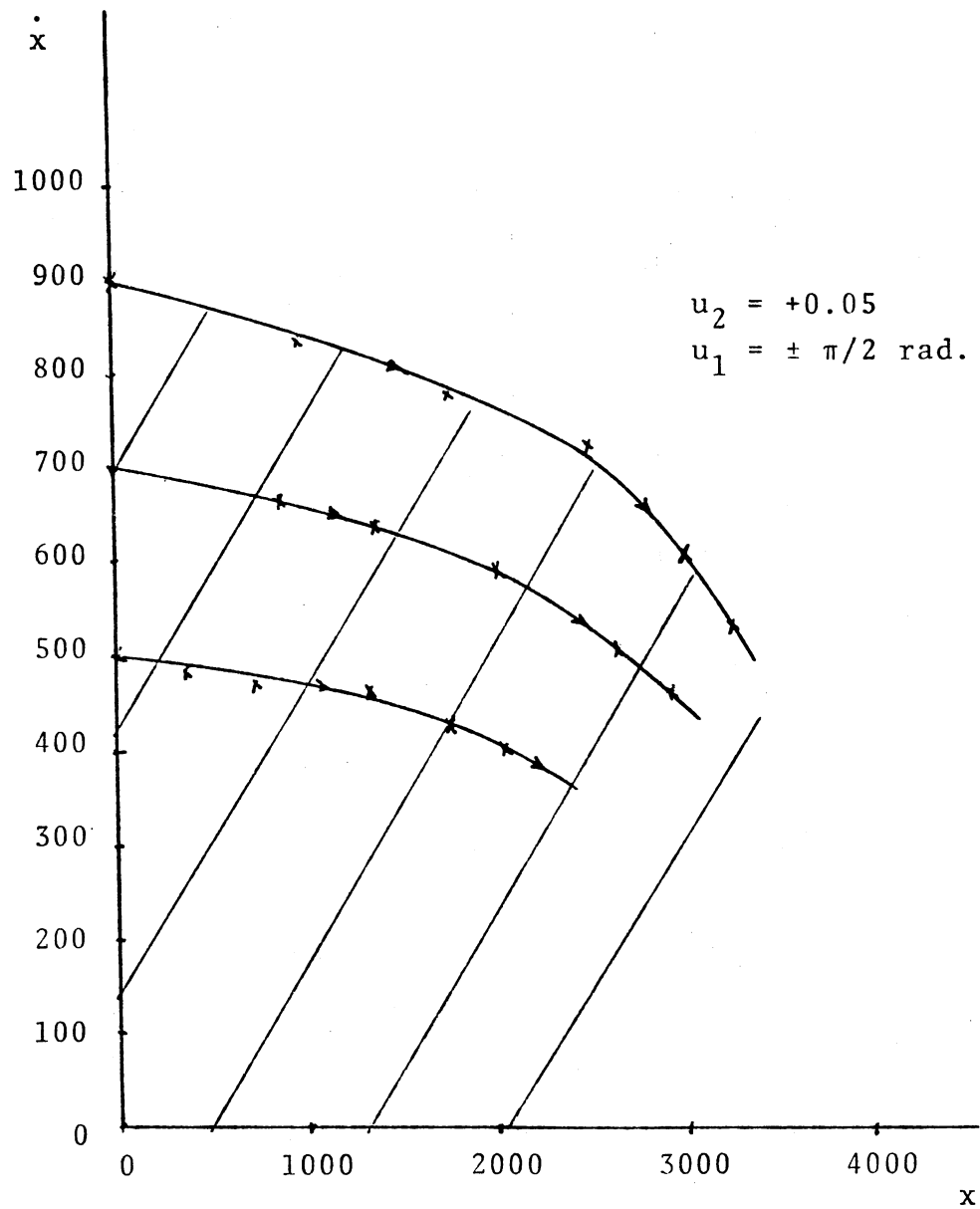


Figure 11. Phase-Plane Trajectories for $u_2 = +0.05$

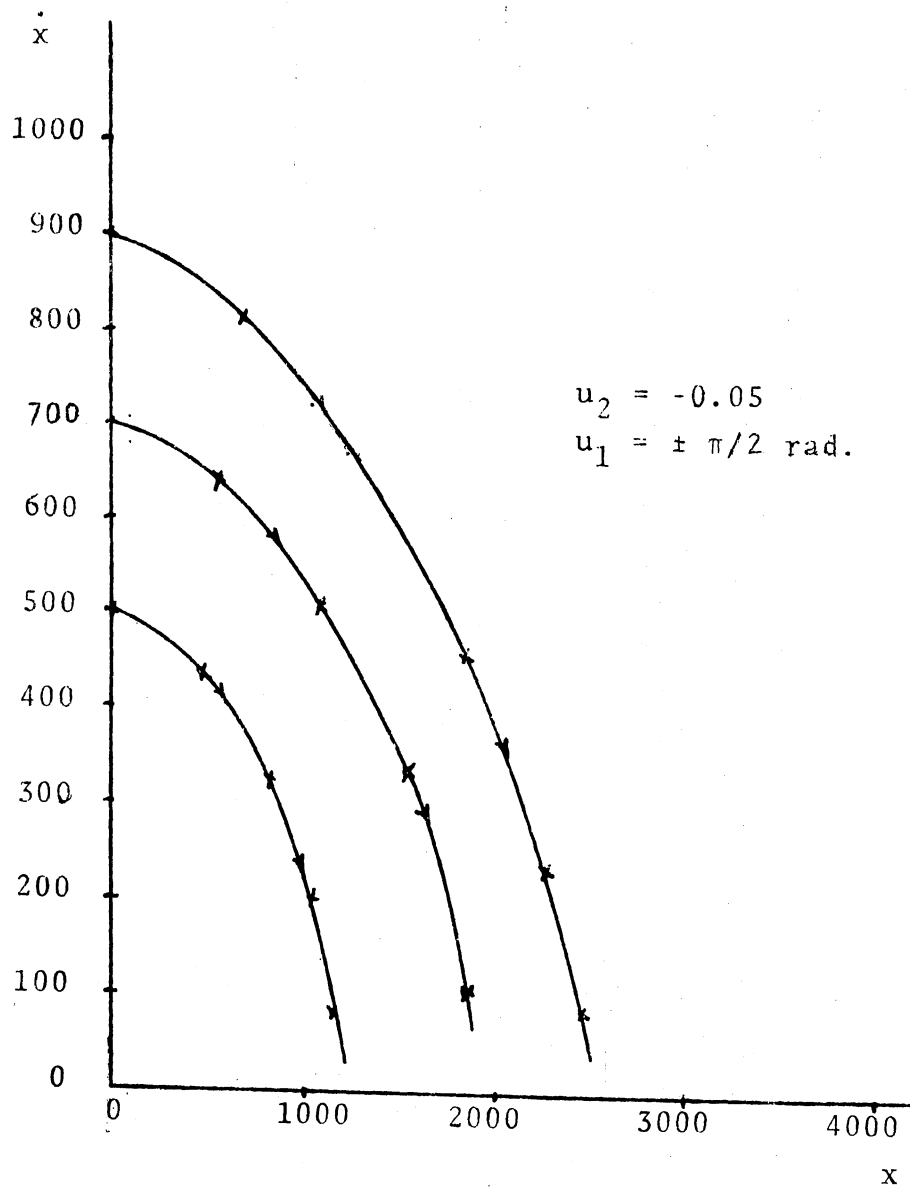


Figure 12. Phase-Plane Trajectories for $u_2 = -0.05$

If a target aircraft has a position and velocity within the shaded area of Figure 11, then it can be intercepted by the attacker aircraft. If the target aircraft trajectory lies outside the shaded area, then it is either moving too fast to intercept or it is too far away to intercept. Since the present model is a relatively short-range model, the latter considerations are not applicable and the target aircraft can thus be intercepted in the x-plane if the position and velocity are known. This result agrees with that found in the minimum-time formulation of a general system of equations.

Figure 13 provides an example of controlling the aircraft trajectory to intercept a given point. If it is desired to intercept a target traveling at 310 feet per second at a distance of 2,600 feet and the attacker has an initial velocity of 700 feet per second, then a suitable suboptimal minimum-time solution is to apply an angle-of-attack rate input of 0.05 radians per second for the first half-second of flight, then apply no control until 2.9 seconds. At this time, apply an angle-of-attack rate of -0.05 radians per second for one-half second and the no control until intercept, which will occur at 4.5 seconds.

Stochastic Regulator Model Results

When attempting to apply the method developed in Chapter II to the real-world formulation of a pilot model, it is important to understand the underlying concepts of the stochastic regulator model. Intuitively, making the time-average of the distance small in $J_K(\underline{u})$ as given by Equation 3.5 makes the probability term of $J(\underline{u})$ as given by Equation 3.2 large. Also, the control energy terms of $J_K(\underline{u})$ and $J(\underline{u})$

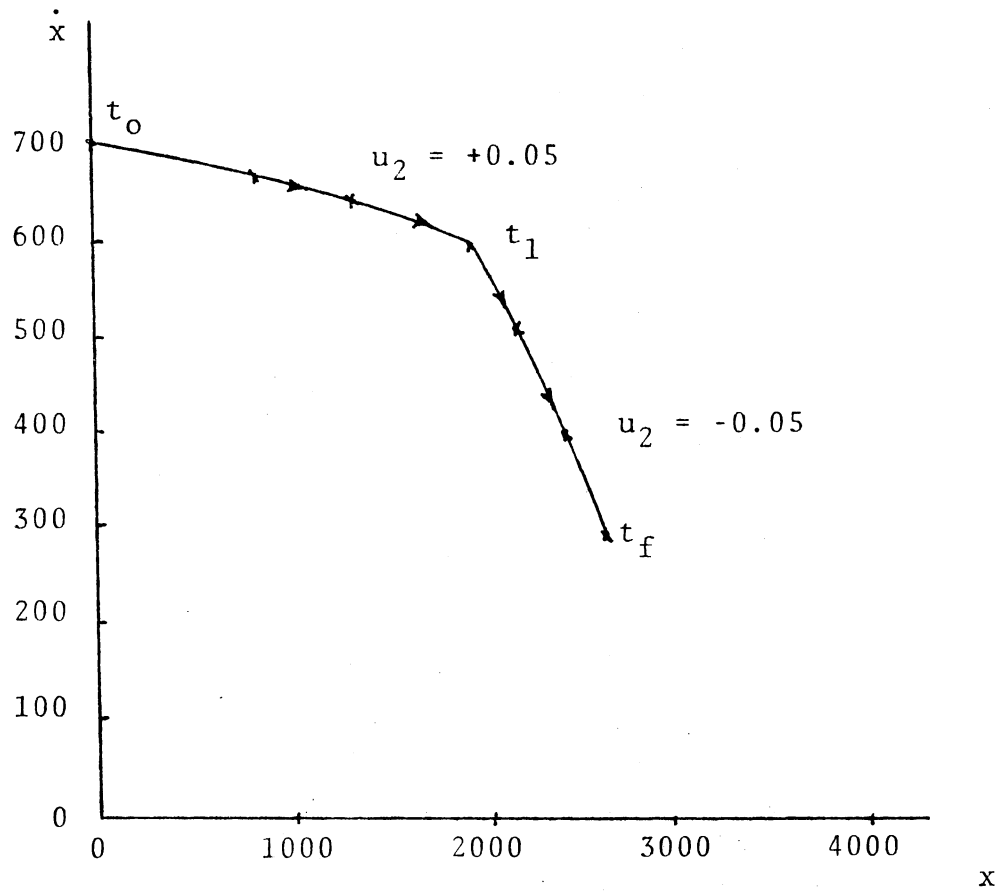


Figure 13. A Suboptimal Trajectory with Switching at Time t_1

are the same if

$$K = \max_i \max_j \max_{t_0 \leq t \leq t_f} |U_{ij}(t)| .$$

In $J_K(\underline{u})$, however, K is the parameter which determines the relative weight placed on the two terms of $J_K(\underline{u})$. Thus, K provides an adjustment of the relative importance of control energy expenditure to state trajectory minimization. It was also known a priori that $J_K(\underline{u})$ as defined in Equation 3.5 would result in a convenient form for the control $\underline{u}_K(t)$ known as the Riccati controller. Each $\underline{u}_K(t)$ was then found as a function of the parameter K , resulting in a class of sub-optimal controls. Thus, the control obtained in applying the stochastic regulator model is suboptimal in the sense that only a certain class of controls is considered at the outset, namely those controls resulting from the solution of the deterministic system 3.4, subject to minimizing the performance index $J_K(\underline{u})$.

Minimizing time rather than control energy is important in actual combat. If energy were a major concern for a pilot, e.g., if fuel were at a critically low level, then an offensive encounter such as is discussed here would certainly be avoided. Following the reasoning presented above, $J_K(\underline{u})$ for the deterministic model of Equation 3.4, including a minimum time term instead of a minimum energy term, would be given by

$$J_K(\underline{u}) = \int_{t_0}^{t_f} \left\{ \underline{x}^T(t) \tilde{a}^{-1}(t) \underline{x}(t) + K \right\} dt \quad (4.2)$$

where $K > 0$. Assuming that the system modeled by Equation 3.4 is completely controllable, minimizing $J_K(\underline{u})$ results in a bang-bang controller with no singular arcs. If $J_K(\underline{u})$ is written in the form

$$J_K(\underline{u}) = \int_{t_0}^{t_f} \underline{x}^T(t) \tilde{a}^{-1}(t) \underline{x}(t) dt + K(t_f - t_0) ,$$

it is easy to see that K provides a relative measure of the importance of minimizing time as opposed to minimizing the state trajectories.

Considering the system modeled by Equation 4.1 and assuming that the system is completely controllable, it is known from optimal control theory that the optimal control is a bang-bang control consisting of at most five switches from maximum-to-minimum control and minimum-to-maximum control. If we consider only the phase-plane plot of the x -direction and assume at most one switch, then the resulting control is obviously suboptimal.

The heavy line in Figure 14 shows the minimum-time deterministic solution for intercept of the target manifold about the target point z . This solution arises from Equation 4.1 as in Figure 13. Suppose the system modeled by Equation 4.1 is subjected to random noise inputs. Then, analogous to Chapter III, it is desired to determine the control $\underline{u}_K(t)$ resulting from different values of the parameter K in $J_K(\underline{u})$ as given by Equation 4.2. If K is a large number, then minimizing time is relatively more important than minimizing the state trajectories. Thus, from inspection of Figure 14, the control $\underline{u}_K(t)$, for K large, is the deterministic control $\underline{u}(t)$. But, $\underline{u}(t)$ also provides the best chance of entering the target manifold if the state trajectories are subjected to random noise disturbances. Thus, if K is small, implying that target intercept is relatively more important than minimizing time, then the deterministic control $\underline{u}(t)$ still provides the sub-optimal control.

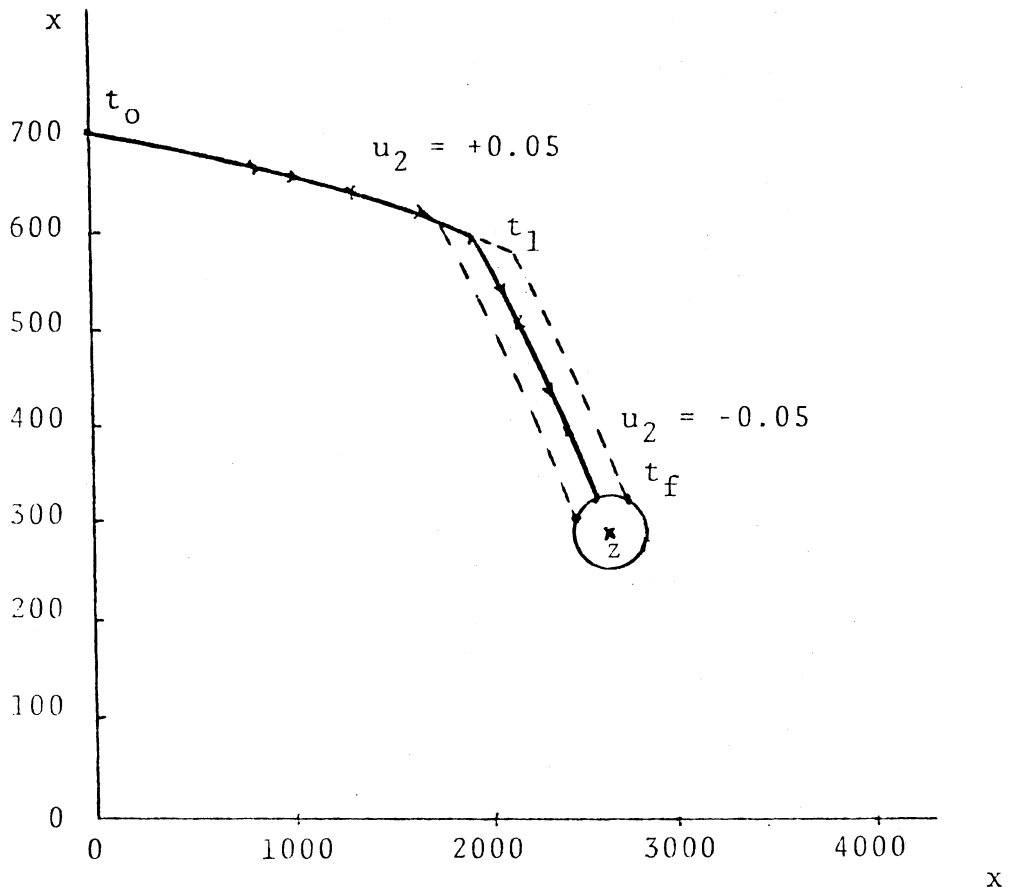


Figure 14. Description of the Stochastic Minimum-Time Trajectory

Summary

It can be concluded, therefore, that if minimizing time is more important than minimizing control energy expenditure for the system modeled by Equation 4.1 subjected to random noise disturbances, then the suboptimal stochastic control is simply the suboptimal deterministic control resulting from minimizing $J_K(\underline{u})$ as given by Equation 4.2. If control energy is to be minimized, then the desired suboptimal control is of the form derived in Chapter III.

CHAPTER V

CONCLUSIONS AND RECOMMENDATIONS

Conclusions

Modern optimal control theory was employed in formulating digital pilot control models for satisfying different performance requirements. First, the problem of target intercept in minimum time was investigated. Assumptions of known target trajectory, implying that the attacking pilot could outguess the target pilot, were inherent in casting the problem in the minimum-time framework. A modified bang-bang control law was found using the minimum-time criterion. This control law was necessarily suboptimal because motion in only one physical dimension was considered. The result was not a true bang-bang controller because maximum control was not applied during the entire time period between the starting time and switching time or between switching time and intercept time.

Next, the optimal controller was found assuming that the attacking pilot did not know beforehand what the target pilot's evasive maneuvers would be. This model incorporated some of the inherent randomness associated with an actual combat situation, along with consideration of control expenditure. The resulting control was a Riccati controller, and it was also a suboptimal control. The suboptimality arose as a result of the problem development in which only

a certain class of controls was considered at the outset.

The suboptimal controller was then found incorporating minimum time as part of the stochastic performance requirement instead of control energy expenditure. The resulting bang-bang control was again suboptimal. It was discovered, however, that the deterministic minimum-time control provided the same result as when the problem was formulated in the stochastic framework with the control energy expenditure term.

If time is more important than control energy, as will generally be the case, then the suboptimal deterministic control is the same as the suboptimal stochastic control. Thus, the considerably simpler bang-bang controller can be found and implemented rather than the somewhat more involved Riccati controller.

Recommendations for Further Study

The control laws derived in this thesis were suboptimal. Optimal control laws could be found for the minimum-time formulation if the geometry associated with several switching possibilities were solved. The optimal control for the stochastic case could be found by investigating the solution of the Kolmogorov diffusion equation. More quantitative information could then be obtained on the relationship of the controls resulting from the different problem formulations.

SELECTED BIBLIOGRAPHY

- (1) Tustin, A. "The Effects of Backlash and of Speed-Dependent Friction on the Stability of Closed-Cycle Control Systems." J. I.E.E., Vol. 94, Part IIA, No. 1, May, 1947.
- (2) A Proposal to Study the Dynamic Characteristics of Man as Related to the Man-Aircraft System, Goodyear Aircraft Corp., Report No. GER-3006-A, May, 1950.
- (3) Human Dynamic Study, Goodyear Aircraft Corp., Report No. GER-4750, April, 1952.
- (4) Seckel, E., I. A. M. Hall, Duane T. McRuer, and D. H. Weir. Human Pilot Dynamic Response in Flight and Simulator, WADC-TR-57-520, October, 1957.
- (5) Hall, I. A. M. Effects of Controlled Element on the Human Pilot, WADC-TR-57-509, August, 1958.
- (6) Hall, I. A. M. "Study of the Human Pilot as a Servo-Element." J. Royal Aeron. Soc., Vol. 67, No. 630, June, 1963.
- (7) McRuer, Duane T., and E. S. Krendel. Dynamic Response of Human Operators, WADC-TR-56-524, October, 1957.
- (8) Kuehnel, Helmut A. Human Pilots' Dynamic-Response Characteristics Measured in Flight and on a Nonmoving Simulator. NASA TN D-1229, 1962.
- (9) McRuer, Duane T., and E. S. Krendel. "The Human Operator as a Servo-System Element." J. Franklin Inst., Vol. 267, No. 5, May, 1959; No. 6, June, 1959.
- (10) Elkind, J. I. Characteristics of Simple Manual Control Systems, M.I.T., Lincoln Lab., TR-111, April, 1956.
- (11) Westbrook, C. B., and Duane T. McRuer. "Handling Qualities and Pilot Dynamics." Aerospace Engineering, Vol. 18, No. 5, May, 1959.
- (12) Ashkenas, I. L., and Duane T. McRuer. "A Theory of Handling Qualities Derived from Pilot-Vehicle System Consideration." Aerospace Engineering, Vol. 21, No. 2, February, 1962.

- (13) Adams, J. J., and H. P. Bergeron. Measured Variation in the Transfer Function of a Human Pilot in Single Axis Tasks. NASA TN D-1952, 1963.
- (14) Anderson, R. O. A New Approach to the Specification and Evaluation of Flying Qualities. AFFDL-TR-69-120, June, 1970.
- (15) McRuer, Duane T., and D. Graham. Human Pilot Dynamics in Compensatory Systems. AFFDL-TR-65-15, July, 1965.
- (16) Krendel, E. S., and Duane T. McRuer. "A Servomechanism Approach to Skill Development." J. Franklin Inst., Vol. 269, No. 1, January, 1960.
- (17) McRuer, Duane T., I. L. Ashkenas, and C. L. Guerre. A Systems Analysis View of Longitudinal Flying Qualities. WADD-TR-60-43, January, 1960.
- (18) Durand, T. S., and H. R. Jex. Handling Qualities in Single-Loop Roll Tracking Tasks: Theory and Simulator Experiments. ASD-TDR-62-507, August, 1962.
- (19) Durand, T. S., and G. L. Teper. An Analysis of Terminal Flight Path Control in Carrier Landings. Systems Technology, Inc., TR-137-1, November, 1964.
- (20) Frost, G. G. An Application of a Dynamic Pilot Model to System Design. ASD-TN-61-57, April, 1961.
- (21) Muckler, F. A., and R. W. Obermayer. The Use of Man in Booster Guidance and Control. AIAA Paper 63-317, August, 1963.
- (22) Smith, R. H. "On the Limits of Manual Control." I.E.E.E. Trans., Vol. HFE-4, No. 1, September, 1963.
- (23) McRuer, Duane T., and E. S. Krendel. Mathematical Models of Human Pilot Behavior. AGARD-AG-188, January, 1974.
- (24) McRuer, Duane T., I. L. Ashkenas, and D. Graham. Aircraft Dynamics and Automatic Control. Princeton Univ. Press, Princeton, J. J., 1973.
- (25) Baron, S., D. L. Kleinman, et al. Application of Optimal Control Theory to the Prediction of Human Performance in a Complex Task. AFFDL-TR-69-81, March, 1970.
- (26) Kleinman, K. L., S. Baron, and W. H. Levison. "An Optimal Control Model of Human Response, Parts I and II." Automatica, Vol. 6, No. 3, May, 1970.
- (27) Kleinman, D. L., S. Baron, and W. H. Levison. "A Control Theoretic Approach to Manned-Vehicle Systems Analysis." I.E.E.E. Trans., Vol. AC-16, No. 6, December, 1971.

- (28) Kleinman, K. L., and S. Baron. Manned Vehicle Systems Analysis by Means of Modern Control Theory. NASA-CR-1753, June, 1971.
- (29) O'Connor, G. E., and J. Y. S. Luh. "Suboptimal Controls that Maximize the Probability of Entering a Target Manifold." I.E.E.E. Trans., Vol. AC-13, No. 6, December, 1968.

VITA

John Mark Richardson

Candidate for the Degree of

Master of Science

Thesis: DEVELOPMENT OF A DIGITAL PILOT CONTROL MODEL

Major Field: Electrical Engineering

Biographical:

Personal Data: Born in Duncan, Oklahoma, April 27, 1954, the son of Mr. and Mrs. Cecil R. Richardson.

Education: Graduated from Duncan High School, Duncan, Oklahoma, in May, 1972; received Bachelor of Science degree in mathematics from Oklahoma State University in December, 1975; completed requirements for Master of Science degree in Electrical Engineering in May, 1977.

Professional Experience: Undergraduate and Graduate Research Assistant, School of Electrical Engineering, Oklahoma State University, beginning in June, 1975.

Professional Organizations: Member of the Institute of Electrical and Electronics Engineers.